Under review, IEEE Trans. PAMI, March 2009

Latent Fingerprint Matching

Anil K. Jain, *Fellow, IEEE,* and Jianjiang Feng

Abstract

Latent fingerprint identification is of critical importance to law enforcement agencies in identifying suspects. While tremendous progress has been made in plain and rolled fingerprint matching, latent fingerprint matching continues to be a difficult problem. Latent fingerprints are inadvertent impressions left by fingers on surfaces of objects. Poor quality of ridge impressions, small finger area and large non-linear distortion are the main difficulties in latent fingerprint matching, compared to plain or rolled fingerprint matching. We propose a system for matching latent fingerprints to rolled fingerprints that is needed in forensics applications. In addition to minutiae, we also use extended features, including singularity, ridge quality map, ridge flow map, ridge wavelength map and skeleton. Our system was tested by matching 258 latents in NIST SD27 database against a background database of 29,257 rolled fingerprints obtained by combining NIST SD4, SD14 and SD27 databases. The minutiae-based baseline rank-1 identification rate of 34.9% was improved to 74% when extended features are used. In order to evaluate the relative importance of each extended feature, these features are incrementally used in the order of their cost in marking by latent experts. The experimental results indicate that singularity, ridge quality map and ridge flow map are the most effective features in improving the matching accuracy.

Index Terms

Fingerprint, minutiae, latent, descriptor, matching, forensics, extended features

I. Introduction

Automated Fingerprint Identification Systems (AFIS) have played an important role in many forensics and civilian applications. There are two main types of searches in forensics AFIS:

Anil K. Jain and Jianjiang Feng are with Department of Computer Science and Engineering, Michigan State University, East Lansing, MI-48824, U.S.A.

E-mail: jain,jfeng@cse.msu.edu

A preliminary version of this paper is contained in [1].

(a) (b) (c)

Fig. 1. Three types of fingerprint images. (a) Rolled, (b) plain and (c) latent fingerprints from the same finger in NIST SD27 [5].

tenprint search and latent search [2]. In tenprint search, the rolled or plain fingerprints of ten fingers of a subject are searched against the fingerprint database of known persons. In latent search, a latent print developed from a crime scene is searched against the fingerprint database of known persons. It is the matching between latents and rolled/plain fingerprints that is of utmost importance to apprehend suspects in forensics. Figure 1 shows fingerprint images of three categories, namely, rolled, plain and latent. Rolled fingerprint images are obtained by rolling a finger from one side to the other ("nail-to-nail") in order to capture all the ridge-details of a finger. Plain impressions are those in which the finger is pressed down on a flat surface but not rolled. While plain impressions cover a smaller area than rolled prints, they typically do not have the distortion introduced during rolling. Rolled and plain impressions are obtained either by scanning the inked impression on paper or by using live-scan devices. Since rolled and plain fingerprints are acquired in an attended mode, they are typically of good quality and are rich in information content. In contrast, latent fingerprints are lifted from surfaces of objects that are inadvertently touched or handled by a person through a variety of means ranging from simply photographing the print to more complex dusting or chemical processing [3], [4].

Latent fingerprints obtained from crime scenes have served as crucial evidence in forensic identification for more than a century. While the wide deployment of Automated Fingerprint Identification System (AFIS) in law enforcement agencies has significantly improved the accuracy and throughput of fingerprint identification, manual intevention is still necessary in latent feature extraction and verification stages. The manual latent identification process can be divided into four steps, namely, analysis, comparison, evaluation and verification. This process is commonly referred to as the ACE-V procedure in latent fingerprint literature [6].

1) Analysis refers to assessing the latent fingerprint to determine whether sufficient ridge information is present in the image to be processed and to mark the features along with the associated quality information. The latent print analysis is usually performed manually by a human expert (without access to a reference print).
2) Comparison refers to the stage where an examiner compares a latent image to a reference print to ascertain their similarity or dissimilarity. Fingerprint features at all three levels (Level 1, Level 2 and Level 3) are compared at this stage.
3) Evaluation stage refers to classifying the fingerprint pair as individualization (identification or match), exclusion (non-match) or inconclusive.
4) Verification is the process of re-examination of a fingerprint pair independently by another examiner in order to verify the results of the first examiner.

It is often argued that matching a latent fingerprint to a rolled print is more of an “art” than “science” [7], [8] because the matching is based on subjective appraisal of the two fingerprints in question by a human examiner. Moreover, the decisions made by latent examiners are required to be “crisp”, i.e., an examiner is expected to provide only one of the three decisions, viz., individualization (identification or match), exclusion (non-match) and inconclusive [3], [4].

There are two types of mistakes a latent examiner can make: false reject and false accept. A false reject occurs when the subject’s rolled/plain fingerprints are actually in the database but the latent examiner fails to identify the latent. A false accept occurs when a latent fingerprint is incorrectly matched to the fingerprint of another subject by the latent examiner. The consequence of false rejects is that criminals may not be apprehended. On the other hand, the consequence of false accepts is that wrongful convictions of innocent persons may occur. While false rejects may be ascribed to poor image quality, false accepts are generally deemed as serious mistakes. However, there is no published research evidence on error rates of latent examiners [9]. One of the most high profile cases in which a false accept was made involves Brandon Mayfield who was wrongly apprehended in the Madrid train bombing incident after a latent fingerprint obtained from the bombing site was incorrectly matched with his fingerprint in the FBI's IAFIS database [10]. Similar cases have been brought to light by the Innocence project [11], [12]. These incidents and findings have undermined the importance of latent fingerprints as forensic evidence. This is evident from a recent ruling of a Baltimore court [13] which excluded fingerprints as evidence in a murder trial because the prosecutor was not able to justify the procedure followed in latent fingerprint matching as being sufficiently error free.

Latent examiners face a huge backlog of cases and are usually under time pressure to evaluate a fingerprint pair, particularly in high profile cases. Therefore, it is very important that the cases sent to latent examiners be carefully selected and prioritized so that he/she can spend adequate amount of time in matching them. One way to achieve this goal is to design an efficient and highly accurate automatic latent to rolled print matching system which is able to provide a quantitative estimate of the probability that two fingerprints being compared belong to the same finger.

In order to deal with throughput issue, the concept of "Lights-Out System" for latent matching has been introduced [14]. A Lights-Out System for fingerprint identification is characterized by a fully automatic (no human intervention) identification process. Such a system should automatically extract features from query fingerprints (latents) and match them with a gallery database (rolled, plain or even latent images) to obtain a set of possible "hits" with high confidence so that no human intervention is required. But due to the limitations of the available algorithms, only "Semi Lights-Out Systems" are feasible especially for latent prints. In a Semi-Lights-Out System some human intervention is allowed during feature extraction from a latent, e.g. orienting the fingerprint, marking the region of interest, etc. The system then outputs a list of candidates that need to be examined by a latent examiner to accept or reject a fingerprint pair as a match.

Although tremendous progress has been made in improving the speed and accuracy of AFIS, these systems work extremely well only in scenarios where the matching is performed between rolled or plain fingerprint images. The results of Fingerprint Vendor Technology Evaluation (FpVTE) [15] showed that the most accurate commercial fingerprint matchers achieved an impressive rank-one identification rate of more than 99.4% on a database of $10,000$ plain

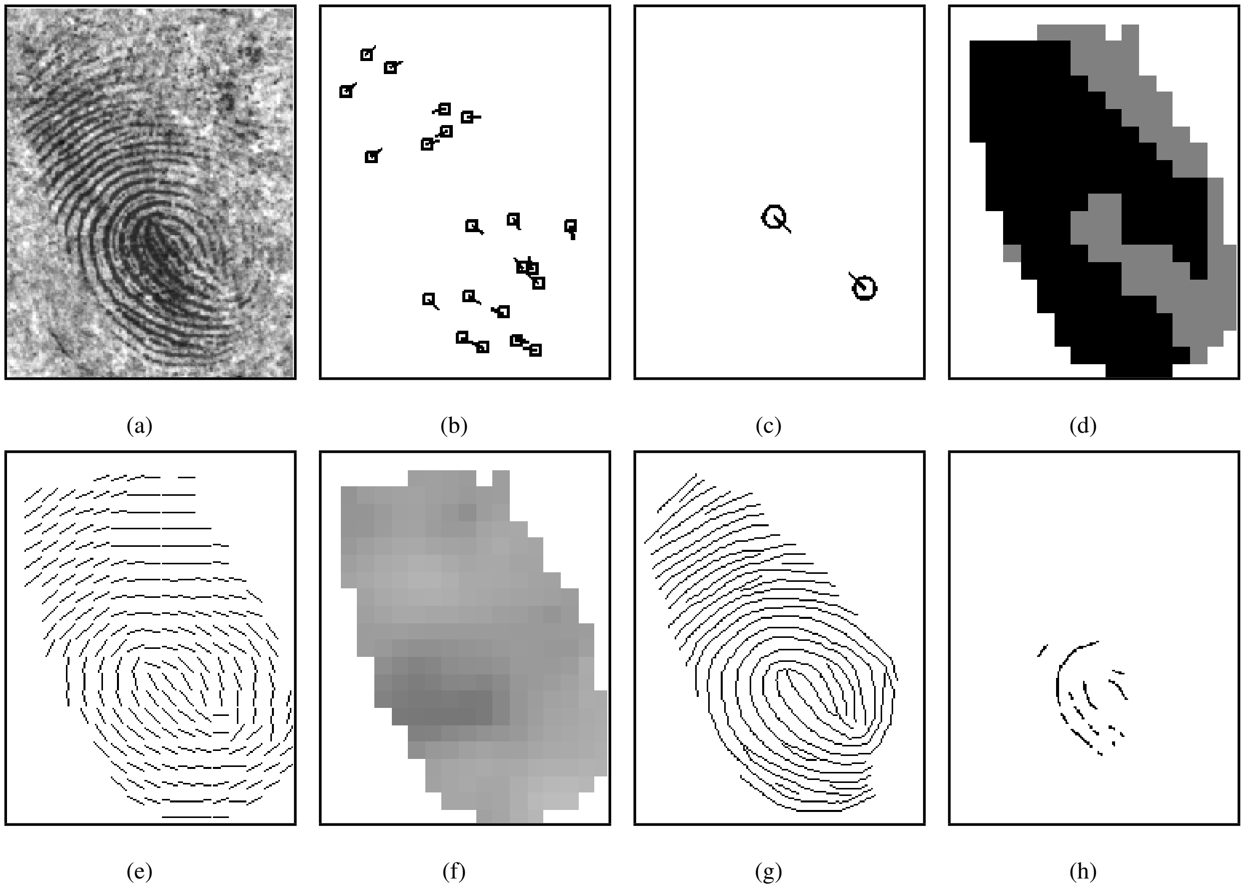

Fig. 2. Features in a latent fingerprint. (a) Grayscale image, (b) minutiae, (c) singular points (cores), (d) ridge quality map (darkness indicates high quality level), (e) ridge flow map, (f) ridge wavelength map, (g) skeletonized image, (h) dots and incipient ridges.

fingerprint images (see results of Medium Scale Test on page 56 in [15]). On the other hand, the NIST latent fingerprint testing workshop reported that the rank-one accuracy of an automatic latent matcher can be as low as 54% on a large database of more than 40 million subjects [14]. NIST is conducting a multi-phase project on Evaluation of Latent Fingerprint Technologies (ELFT) [16]; phase-I results showed that the best latent fingerprint matcher had an identification accuracy of 80% in identifying 100 latent images among a database of 10,000 rolled prints. This accuracy is significantly lower than the accuracy of rolled print to rolled print matching on a similar size database.

The difficulty in latent matching is mainly due to three reasons: 1) poor quality of latent prints in terms of the clarity of ridge information, 2) small finger area in latent prints as compared to rolled prints and 3) large non-linear distortion due to pressure variations. Figure 1 shows a sample latent image from the NIST SD27 along with its mated plain and rolled prints. The ridge structure of the latent image is obscured and there exists another latent print below it. Further, while a typical rolled fingerprint has around 80 minutiae, a typical latent fingerprint may have only 15 usable (reasonable quality) minutiae.

To improve the accuracy of latent matching algorithms, in addition to minutiae, additional features have to be used, as is typically done by latent examiners in the ACE-V procedure [6]. Fingerprint features are generally categorized into three levels:

1) Level 1 features are the macro details of the fingerprint such as ridge flow, singular points, and pattern type.
2) Level 2 features refer to ridge skeletons, ridge bifurcations and endings (namely minutiae) , dots, and incipient ridges.
3) Level 3 features include ridge contours and pores whose robust extraction needs high resolution images ($\geq$ 1,000 ppi) compared to the current FBI standard of 500 ppi.

Fingerprint features other than minutiae and singular points are collectively referred to as extended features [17], as they are not included in the current fingerprint standard [18]. See Fig. 2 for various features in a latent fingerprint.

In this paper, we propose a latent-to-rolled/plain matching algorithm which utilizes minutiae, reference points (core, delta, and center point of reference), overall image characteristics (ridge quality map, ridge flow map, and ridge wavelength map), and skeleton (or skeletonized image). These features are chosen due to their distinctiveness, repeatability, universality, and detectability in 500 ppi fingerprint images. The features are manually marked for latents, but they are automatically extracted for rolled prints and the matching algorithm is also automatic. A rank-1 identification rate of 74% was obtained in matching 258 latent images in NIST SD27 [5] against a background database of 29,257 rolled prints, which is composed of NIST SD27 [5] (257 fingerprints after removing a duplicate image), NIST SD4 [19] (2,000 file fingerprints) and NIST SD14 [20] (27,000 file fingerprints).

Another goal of this study is to understand the relative importance of various extended features which will benefit fingerprint standardization in forensic and governmental applications. It is widely realized that template standardization is very important for biometric industry. Adoption of standard templates is especially important for law enforcement applications, since it is very common for latent examiners to encode (extract features) latent prints using their own AFIS and then submit them to another AFIS (by a different vendor) for matching. Improving AFIS interoperability has been listed as one of the thirteen recommendations by the NAS Committee on Identifying the Needs of the Forensic Science Community [21] to address the most important issues now facing forensic science community. The FBI Electronic Fingerprint Transmission Specification (EFTS) [22], which is mainly based on minutiae, has served as the fingerprint standard in the forensic community in the United States. Although AFIS vendors may use additional features in searching latents encoded by their own AFIS [23], [24], only minutiae are involved in searching latents encoded by AFIS from different vendors. This leads to significant degradation in matching accuracy and limits the interoperability between different AFIS systems. This phenomenon has been observed in the NIST Minutiae Interoperability Exchange Test (MINEX) [25] and Proprietary Fingerprint Template (PFT) Testing [26], where the standard minutiae template produces lower matching accuracy than the proprietary templates. This suggests that current minutiae standard should be extended to include additional features that can be used to improve AFIS interoperability. In the 2005 ANSI/NIST fingerprint standard update workshop [27], the Scientific Working Group on Friction Ridge Analysis, Study and Technology (SWGFAST) [28] recommended that extended features be included in the FBI fingerprint standard. This recommendation was endorsed by the forensic community and it initiated the establishment of an ANIS/NIST committee, named the ANSI/NIST Committee to Define an Extended Fingerprint Feature Set (CDEFFS), to define an extended fingerprint feature set [17]. The current CDEFFS document [29] includes several extended features (e.g., ridge flow map, skeletonized image, ridge quality map, virtual reference point, crease, dot, incipient ridge, pore). However, it may not be practical for latent examiners to mark all the available features in latents, due to their heavy workload and backlog. It is also impractical for fingerprint vendors to develop robust algorithms for all the extended features. Thus it is prudent to first examine the performance gain resulting from various extended features in latent matching and understand the relative importance of these extended features. With this information, latent examiners may mark only salient features and vendors can put more effort on these features. Furthermore, this will allow CDEFFS to make the definitions of salient features more precise. To achieve this goal, various extended features are incrementally used in our matching algorithm and the performance gains are compared. The order of adding extended features to the matching process is based on their cost in manual marking and their detectability in 500 ppi fingerprint images. For example, ridge flow map is used ahead of ridge skeleton since the former needs less effort in manual feature marking.

A. Related Work

It is a common practice to improve the capability of minutiae matcher by using Level 1 and Level 2 features. These include singular points and pattern type [23], ridge flow map (or orientation field) [23], [30]–[34], ridge wavelength map (or frequency map) [30], [35], skeleton [23], [24], [30], [36], [37], and crease [38]. We have also utilized these Level 1 and Level 2 features for latent fingerprint matching.

There is a growing interest in using Level 3 features, such as pores [34], [39], [40], ridge contours [34], [40], dots and incipient ridges [41], for fingerprint matching. It is claimed that Level 3 features contain discriminating information and can improve the performance of matching rolled/plain to rolled/plain fingerprints. However, these conclusions are not easy to extend to latent fingerprint matching, because

- Latent fingerprints are generally of poor quality.
- Since latent images need to be matched against rolled/plain fingerprints, the repeatability or consistency of Level 3 features is critical. Repeatability of Level 3 features in images acquired with different techniques is much lower than that in [34], [40], [41] where the same sensor was used to capture both template and query fingerprints.
- Level 3 features such as pores and ridge edges are correlated with skeleton and ridge flow map. Therefore, it is not evident if the performance improvement reported in [34], [40], [41] is due to Level 3 features or Level 2 features that have been implicitly used.

II. Feature Extraction

A. Features

The proposed system utilizes the following features [29]: reference points (singularity), overall image characteristics (ridge quality map, ridge flow map, and ridge wavelength map), minutiae, and skeleton. The effect of the secondary features (dots, incipient ridges, and pores) has also been examined. Since all these features are defined in the CDEFFS document [29], we use terms that are consistent with these definitions. Note that not all the features and all the properties for each feature defined in [29] have been implemented in our system.

- Reference points have location, direction and type (see [29]).
- Ridge flow map, ridge wavelength map and ridge quality map are obtained by dividing the image into non-overlapping bocks of size 16×16 and assigning a single orientation, wavelength and quality value to each block. We define three quality levels for a block: level 0 (background), level 1 (clear ridge flow and unreliable minutiae) and level 2 (clear minutiae).
- A minutia consists of five attributes, namely x and y coordinates, minutiae direction, type and quality. The quality of minutia is defined to have two levels: 0 (unreliable) and 1 (reliable).
- A skeleton is one-pixel-wide ridge, which is traced in the thinned image and represented as a list of points.
- Secondary features (dots, incipient ridges, and pores) are represented as a set of points.

While these features have been manually marked for 258 latents in SD27, the rolled fingerprints are automatically processed to obtain all the features, except for the secondary features (dots, incipient ridges, and pores), which are manually marked. The feature extraction algorithm consists of two modules: preprocessing and postprocessing. In this work, Neurotechnology Verifinger 4.2 SDK [42] was used as a preprocessor. Due to the presence of background noise (characters and strokes on many fingerprints scanned from paper, such as the rolled prints in NIST SD4, SD14, and SD27), Verifinger produces many false minutiae. Therefore, a minutiae validation algorithm and a ridge validation algorithm are used to classify minutiae as false, reliable or unreliable, and ridges as either true or false, respectively. The other features are generated based on the validated ridges. The results of the various processing steps are shown in Fig. 3.

B. Minutia and Ridge Validation

A minutia is deemed as false if it is close to the background region. A minutia is deemed as unreliable if it forms an opposite pair with another minutia. An opposite pair is a pair of minutiae which are spatially close but have opposite directions. Remaining minutiae are deemed as reliable. These rules are similar to the rules used in [43].

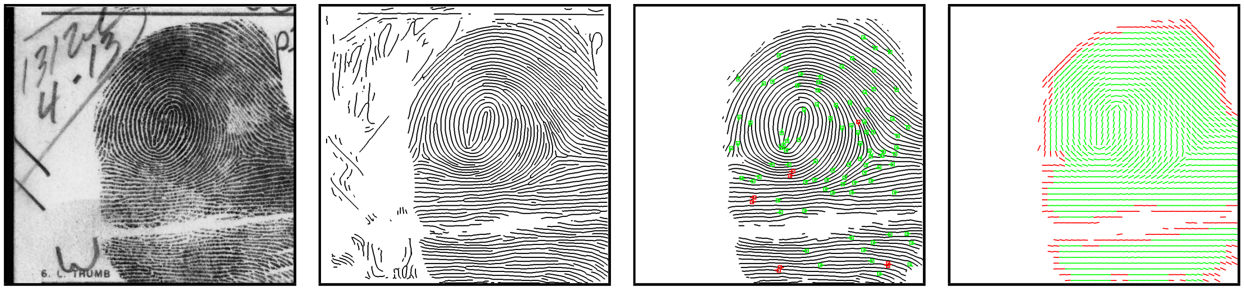

(a) (b) (c) (d)

Fig. 3. Feature extraction in a rolled fingerprint. (a) Gray image, (b) thinned image, (c) ridges and minutiae (green: reliable minutiae, red: unreliable minutiae), (d) ridge flow map and ridge quality map (green: reliable blocks, red: unreliable blocks).

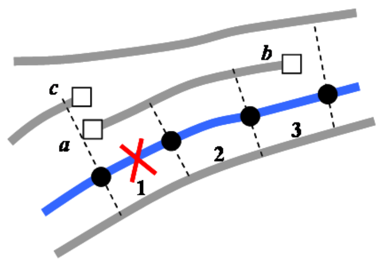

Fig. 4. Reliability of a ridgel. Ridgel 1 is unreliable due to an unreliable minutia a. Both ridgels 2 and 3 are reliable.

Ridge validation consists of the following two steps: 1) each ridge is broken into multiple segments at unreliable positions; 2) the segments are grouped and those belonging to large groups are deemed as reliable. In the first step each ridge is broken into several segments at unreliable ridgels (ridgels are defined as adjoining sequences of six consecutive pixels on a ridge). Reliability of a ridgel is based on neighboring ridge pixels of the two endpoints of the ridgel (see Fig. 4). A ridgel is called reliable if 1) the neighboring ridge pixels on both sides are continuous, or 2) discontinuity in neighboring ridge pixels is caused by a reliable minutia (such as minutia b in Fig. 4). In the second step two ridges are deemed compatible if there are more than 12 pixels on each ridge that are neighbors of each other. The connected components (ridge groups) are then found using a depth-first search algorithm. A ridge group is deemed reliable if the number of ridge pixels in this group is greater than a predefined threshold ($1,000$ in our experiment). The ridges in a reliable group are deemed as true and other ridges are deemed as false. Minutiae associated with false ridges are deemed as false.

C. Generation of Other Features

A block containing true ridges is labeled as foreground; otherwise as background. For each sample point (at intervals of 6 pixels) on each ridge, the tangent direction is computed and the distance from the adjacent ridges on both sides is computed. The ridge flow and ridge wavelength in each foreground block are estimated by majority voting. Singular points are extracted by the Poincaré index method [44].

III. MATCHING

To understand the relative importance of various extended features, they are incrementally used for matching and the performance gains are examined. Starting with the baseline matching algorithm, which uses only minutiae, reference points, overall image characteristics and skeleton are incrementally used. This order is based on their cost in manual marking.

A. Baseline Matching Algorithm

The baseline matching algorithm takes only minutiae as input and consists of the following steps:

1) Local minutiae matching: Similarity between each minutia of latent fingerprint and each minutia of rolled fingerprint is computed.
2) Global minutiae matching: Using each of the five most similar minutia pairs found in Step 1 as an initial minutia pair, a greedy matching algorithm is used to find a set of matching minutia pairs.
3) Matching score computation: A matching score is computed for each set of matching minutia pairs and the maximum score is used as the matching score between the latent and rolled prints.

1) Local Minutiae Matching: In this step, the similarity between each minutia of latent fingerprint and each minutia of rolled fingerprint is computed. Since the basic properties of a minutia, like location, direction and type, are not very distinctive features, additional features, which are collectively referred to as a descriptor, are computed for each minutia. Figure 5 show five types of features that have been used as minutiae descriptors in the literature [30], [45], [46]. In the baseline algorithm, a neighboring minutiae-based descriptor is used, since only minutiae information is available.

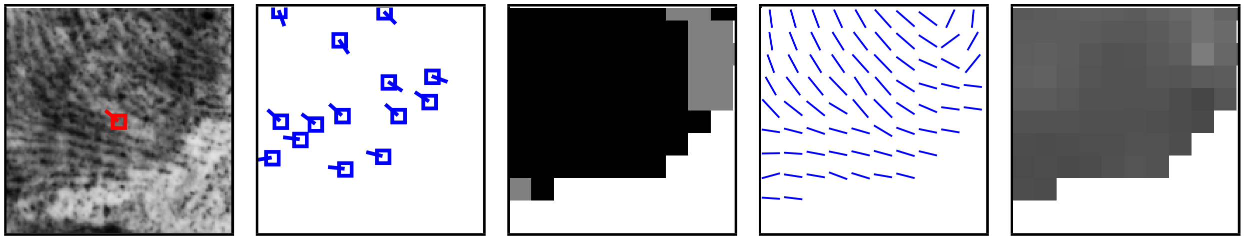

(a) (b) (c) (d) (e)

Fig. 5. Minutia descriptors. (a) Local grayscale image, (b) neighboring minutiae, (c) local ridge quality map, (d) local ridge flow map, and (e) local ridge wavelength map.

The neighborhood of a minutia is defined to be a circular region of radius 80 pixels. All minutiae lying in this neighborhood are called the neighboring minutiae. Let p and q be the two minutiae whose similarity needs to be computed. For each neighboring minutia p_i of p, we examine if there is a neighboring minutia of q whose properties (See Fig. 6) are similar to those of p_i. If such a minutia exists, p_i is deemed as a matching minutia; otherwise p_i is checked against the following two criteria: 1) the minutia is unreliable, 2) it does not fall in the foreground region (the convex hull of minutiae) when mapped to the other fingerprint based on the alignment parameters between p and q. If p_i satisfies either one of these two criteria, it will not be penalized; otherwise, it will be penalized. The above process is also applied to the neighboring minutiae of q. The similarity between two neighboring minutiae-based descriptors is computed as:

$$s_m = \frac{m_p + 1}{m_p + u_p + 3} \cdot \frac{m_q + 1}{m_q + u_q + 3}, \tag{1}$$

where m_p and m_q denote the number of neighboring minutiae of p and q that match, u_p and u_q denote the number of penalized unmatched neighboring minutiae of p and q, the value 1 in the numerator is used to deal with the case where no neighboring minutiae are available, and the value 3 in the denominator is empirically chosen to favor the case where there are more neighboring minutiae that match. Note that m_p may be different from m_q since we do not establish a one-to-one correspondence between minutiae.

2) Global Minutiae Matching: Given the similarity among all minutia pairs, the one-to-one correspondence between minutiae is established in the global minutiae matching stage. Greedy strategy is used to find matching minutia pairs in the decreasing order of similarity. In order to

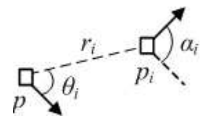

Fig. 6. Properties of neighboring minutia p_i in the local polar coordinate system defined by the central minutia p.

give priority to those minutia pairs that are not only similar to each other but also dissimilar with other minutiae, a normalized similarity measure s_n is defined based on similarity s as:

$$s_n(i,j) = \frac{(N_m^L + N_m^R - 1) \cdot s(i,j)}{\sum_{k=1}^{N_m^R} s(i,k) + \sum_{k=1}^{N_m^L} s(k,j) - s(i,j)} \tag{2}$$

where $s(i,j)$ denotes the similarity between minutia i and minutia j, and N_m^L and N_m^R denote the number of minutiae in the latent and rolled, respectively. All minutia pairs are sorted in the decreasing order of normalized similarity and each of the top 5 minutia pairs is used to align the two sets of minutiae. Minutiae are examined according to the decreasing order of their similarity; minutiae that are close in both location and direction, and have not been matched to other minutiae are deemed as matching minutiae. After all the minutia pairs have been examined, a set of matching minutiae is returned.

3) Matching Score Computation: When fewer than three minutiae are matched, the matching score S_M is set as 0; otherwise S_M is the product of a quantitative score S_{mn} and a qualitative score S_{mq}:

$$S_M = S_{mn} \cdot S_{mq}. \tag{3}$$

The quantitative score S_{mn} is computed as $M_m/(M_m + 8)$, where M_m denotes the number of matched minutiae and the value 8 is an estimate of the average number of matching minutiae for low quality latents. The qualitative score is computed as:

$$S_{mq} = S_d \cdot \frac{M_m}{M_m + U_m^L} \cdot \frac{M_m}{M_m + U_m^R} \tag{4}$$

where S_d is the average similarity of descriptors for all matching minutiae, and U_m^L and U_m^R denote the number of penalized unmatched minutiae (defined in Sec. III-A1) in latent and rolled prints, respectively.

B. Reference Points

Using the spatial transformation between the two images, which is estimated based on the matched minutiae, the reference points (if present) of the latent are transformed into the coordinate system of the rolled print. The distance and angle difference between reference points of the same type are computed and compared to predefined thresholds (30 for distance and $\pi/4$ for angle). If both values are less than their respective thresholds, the reference points are deemed as matched. The accumulated matching score is computed as:

$$S_R = S_M + C_r \cdot S_r, \tag{5}$$

where S_r denotes the matching score based on reference points, namely, the number of matched reference points and C_r is a constant value empirically set as 0.03.

C. Overall Image Characteristics

1) Ridge Quality Map: Ridge quality map is used in local minutiae matching and matching score computation stages to ignore the unmatched minutiae of one fingerprint that are mapped to the low quality region (quality level 0 or 1) of the other fingerprint. As will be shown in Sec. IV, this modification significantly improves the matching accuracy. The accumulated matching score S_Q is computed by Eqs. (3) and (5).

2) Ridge Flow Map: Ridge flow map is used in two stages: local minutiae matching and matching score computation.

For every minutia, a local coordinate system is defined with the minutia as the origin and its direction as the positive x axis. A set of fixed sample points is defined (See Fig. 7) and the local ridge flow at these sample points form the flow descriptor. These sample points are located on four concentric circles centered at the minutia, and distributed equally on each circle. The radii of circles are 27, 45, 63 and 81 and the numbers of sample points on these circles are 10, 16, 22, and 28, respectively. These parameters have been determined empirically in [31]. The similarity of two descriptors is computed as the mean value of the similarity of all valid sample points (a sample point falling in background region is deemed as invalid). The similarity between the flow at two sample points is computed as $s_f = exp(-|\Delta\theta|/(\pi/16))$, where $\Delta\theta$ denotes the angle between the two flows. If the number of common valid sample points is less than 25% of the total number of sample points, the similarity of two minutiae is set to 0. The similarity between

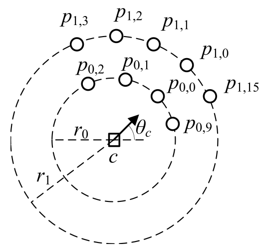

Fig. 7. The configuration of sample points of ridge flow and ridge wavelength based descriptors.

two minutiae is computed as the weighted sum of the neighboring minutiae-based similarity and flow-based similarity:

$$s = w_m \cdot s_m + (1 - w_m) \cdot s_f, \tag{6}$$

where the weight w_m for the neigbhoring minutiae-based descriptor is empirically set as 0.6, due to its superior performance compared to flow-based descriptor.

The ridge flow maps of latent and rolled prints are aligned using the spatial transformation estimated based on the matched minutia pairs. The matching score S_f based on ridge flow is the product of a quantitative score S_{fn} and a qualitative score S_{fq}. The quantitative score S_{fn} is computed as $N_b/(N_b + 100)$, where N_b is the number of blocks where the difference in flow is less than $\pi/8$ and the value 100 is an estimate of the average number of 16×16 blocks in low quality latents. The qualitative score S_{fq} is computed as $(1 - 2 \cdot D_f/\pi)$, where D_f is the mean of the difference of flow values in all overlapping blocks.

The accumulated matching score S_F between two fingerprints is computed as:

$$S_F = S_M + S_R + C_f \cdot S_f, \tag{7}$$

where the constant C_f is empirically set as 0.2.

3) Ridge Wavelength Map: Ridge wavelength map is used in two stages: local minutiae matching and matching score computation.

Wavelength-based minutia descriptor is composed of the ridge wavelength at a set of sample points as shown in Fig. 7. The similarity between the wavelength of two sample points is computed as $s_w = exp(-|\Delta w|/3)$, where Δw denotes the wavelength difference at two sample points. The similarity between two minutiae is computed as the weighted sum of the neighboring minutiae-based similarity, flow-based similarity, and wavelength-based similarity:

$$s = w_m \cdot s_m + w_f \cdot s_f + (1 - w_m - w_f) \cdot s_w, \tag{8}$$

where the weights w_m and w_f for the neigbhoring minutiae-based and flow-based descriptors are empirically set as 0.6 and 0.2, respectively.

The ridge wavelength maps of latent and rolled prints are aligned using the spatial transformation estimated based on the matched minutia pairs. The matching score S_w based on wavelength is the product of a quantitative score S_{wn} and a qualitative score S_{wq}. The quantitative score S_{wn} is computed as $N_b/(N_b + 100)$, where N_b is the number of blocks where the difference in wavelength is less than 3 pixels and the value 100 is an estimate of the average number of 16×16 blocks in low quality latents. The qualitative score S_{wq} is computed as the average similarity of wavelength in all overlapping blocks.

The accumulated matching score S_W between two fingerprints is computed as:

$$S_W = S_M + C_r \cdot S_r + C_f \cdot S_f + C_w \cdot S_w, \tag{9}$$

where the constant C_w is empirically set as 0.2.

D. Skeleton

Minutiae can be deemed as an abstract representation of ridge skeleton. However, the skeleton image contains more information than minutiae. The skeleton matching algorithm is similar in spirit to the "ridges in sequence" idea recommended by SWGFAST [47]. Hara and Toyama [24] describe an interesting skeleton matching algorithm, which consists of the following steps: 1) select the most reliable minutiae pair from all matched minutiae pairs as the base paired minutiae (BPM); 2) remove minutiae pairs that are inconsistent with BPM; 3) modify the two skeleton images to make them more similar; and 4) incrementally match skeleton points guided by the matched minutiae or skeleton points. While their approach needs at least three pairs of correctly matched minutiae to guide the skeleton matching process, our approach needs only a pair of correctly matched minutiae as starting point, which is useful in matching latent prints with very small area.

The proposed skeleton matching algorithm is a modified version of the algorithm in [36], which consists of the following steps: Starting from each of the initial minutiae pairs found by comparing ridge structures associated with minutiae, the correspondence between skeletons is established and a matching score is computed. The maximum value of these scores is used as the skeleton matching score. We modify this algorithm in the following ways. Firstly, initial minutia pairs are found by comparing the composite minutiae descriptor based on neighboring minutiae, ridge flow and wavelength features, which is more accurate than the method in [36]. Secondly, the skeleton matching score is computed as the product of a quantitative score S_{sn} and a qualitative score S_{sq}:

$$S_s = S_{sn} \cdot S_{sq}. \tag{10}$$

The quantitive score S_{sn} is computed as:

$$S_{sn} = \frac{M_s}{M_s + 400}, \tag{11}$$

where the value 400 is an estimate of the average number of skeleton sample points in low quality latents. The qualitative score is computed as:

$$S_{sq} = \frac{M_s}{M_s + U_s^L} \cdot \frac{M_s}{M + U_s^R}, \tag{12}$$

where U_s^L and U_s^R denote the number of unmatched skeleton sample points of latent and rolled prints in their common region, respectively. The accumulated matching score S_S is obtained by combining S_s and S_W computed in Eq. (9):

$$S_S = S_W + C_s \cdot S_s, \tag{13}$$

where the constant C_s is empirically set as 1. For efficiency, skeleton matching is performed only for the top 100 candidates found by the minutiae matcher.

IV. Experimental Results

A. Database

To evaluate the latent fingerprint matching algorithm, 258 latent fingerprints in NIST SD27, which also contains their mated rolled prints, were matched against a large background database of rolled prints. This is the only public domain database available containing mated latent and rolled prints. These 258 latent prints were classified by latent examiners into three classes, namely: Good, Bad and Ugly based on the quality of latent fingerprints in the database. There are 88 Good, 85 Bad and 85 Ugly latent images in SD27. Since there are only 257 (exclude one duplicate image) rolled fingerprints in SD27, to make the latent-to-rolled matching problem more realistic, we expand the background database by adding fingerprints from NIST SD4 and SD14 databases. There are 2,000 different fingers and 2 rolled impressions per finger in SD4, and 27,000 fingers and 2 rolled impressions per finger in SD14. These fingerprints were also scanned from paper and have similar characteristics to the rolled prints in SD27. The 29,000 file fingerprints in SD4 and SD14 are combined with the 257 rolled images in SD27 to form a background database containing 29,257 rolled prints. We search the 258 latents against this background database of 29,257 rolled prints. All these fingerprint images are scanned at 500 ppi.

B. Matching Accuracy

The Cumulative Match Characteristic (CMC) curve of the proposed algorithm in searching all 258 latents against the background database of 29,257 rolled prints is shown in Fig. 8a. A CMC curve plots the rank-k identification rate against k, for $k = 1, 2, \cdots, 20$. The rank-k identification rate indicates the proportion of times the mated fingerprint occurs in the top k matches. A rank-1 identification rate of 74.0% and a rank-20 identification rate of 82.9% were achieved. Note that no systematic procedure has been used to select the best parameters in matching score computation, due to a lack of a large number of latents. The matching accuracy can be further improved by fusing the matching results of latent-to-rolled and latent-to-plain, as shown in [48]. To our knowledge, only ELFT07 [16] has reported matching performance using latents in SD27. ELFT07 tested fully automated latent search technology by searching 100 latents against a background database of 10,000 rolled prints. But, only the average performance over all ten participating vendors is reported in [16]; the average rank-1 rate is about 60% on a background of 10,000 rolled prints and 67% on a background of 1,000 rolled prints. The results of ELFT07 and our results can not be compared directly. In ELFT07 phase I, out of 100 latents only 50 are from SD27, and the quality of these selected latents is unknown. As shown in Fig. 8b, the accuracies for different quality latents are significantly different. The ELFT phase II used a larger database, but the final report is still not available in the public domain.

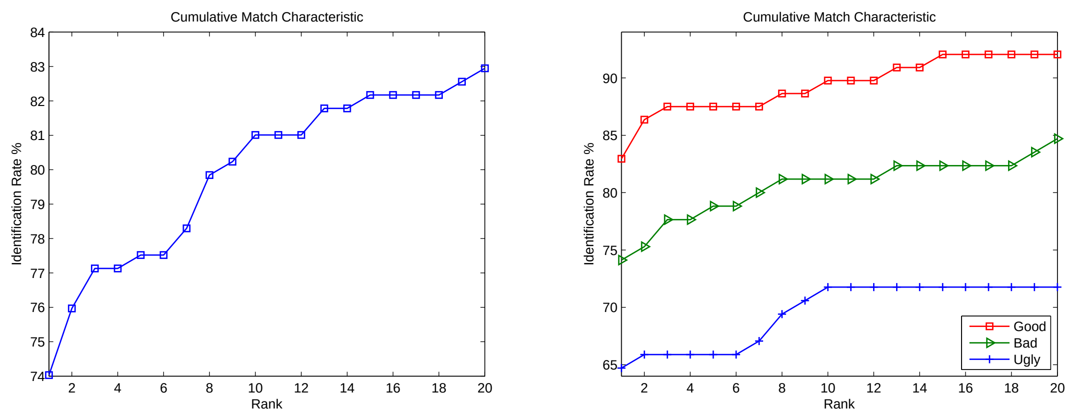

(a) (b)

Fig. 8. CMC curve of the proposed algorithm on a background database of 29,257 rolled prints. (a) All 258 latents, (b) Good, Bad and Ugly quality latent prints. These three categories contain 88, 85 and 85 latents, respectively.

C. Latent Quality

Figure 8b shows the CMC curves of the proposed algorithm separately for Good, Bad and Ugly quality latent prints. As expected, the matching performance for Good quality latents is significantly better than those for the latents belonging to the other two quality groups. Three examples of successful identification (one from each quality group) are shown in Fig. 9. In all these three cases, the mated rolled print was found at rank 1. It should be noted that although there are only 4 matching minutiae in the Ugly latent (Fig. 9), our algorithm still identified it correctly at rank-1. However, if a large number of spurious minutiae are detected in the overlapping region of latent and rolled prints, the matching algorithm will fail as shown in Fig. 10.

D. Importance of Extended Features

Figure 11a plots the rank-1 identification rates for all 258 latents when extended features are incrementally used. The largest accuracy improvement is due to singularity feature; ridge quality map and ridge flow map also significantly improve the matching accuracy. Figure 11b shows the rank-1 identification rates separately for each quality level when extended features are incrementally used. It can be observed that Ugly quality latents benefit the most from the use of extended features. Figure 12 shows the matched minutiae and skeletons between a latent and its

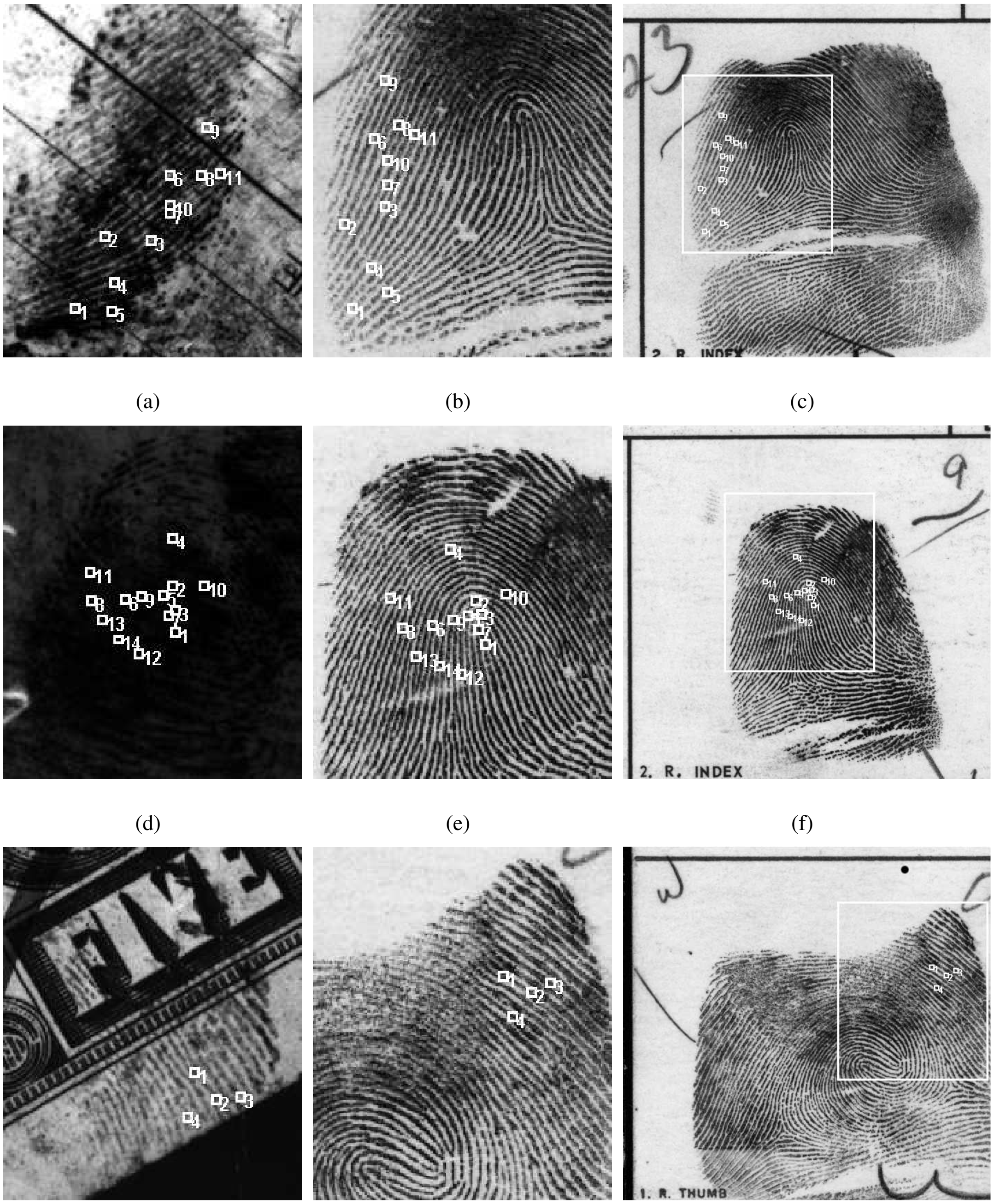

(a) (b) (c)

(d) (e) (f)

(g) (h) (i)

Fig. 9. Examples of successful matchings. Three latents (classified as (a) good, (d) bad and (g) ugly by latent examiners), the corresponding regions in the mated rolled prints ((b), (e), (h)), and the mated rolled prints ((c), (f), (i)). In all these three cases, our algorithm found the true mate at rank one.

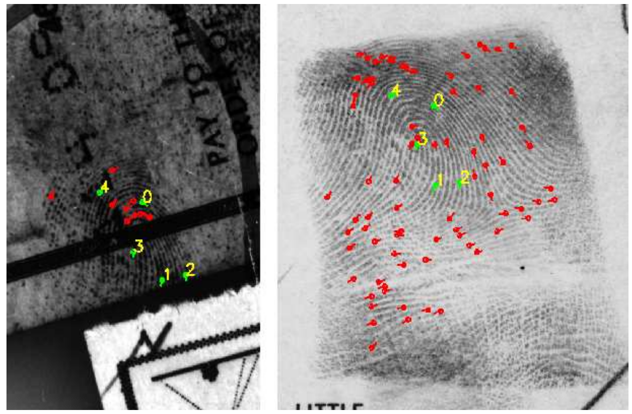

Fig. 10. Example of an incorrect match. The mated rolled print (right) of the latent (left) was ranked 200 by our algorithm. Many spurious minutiae are detected in the rolled print.

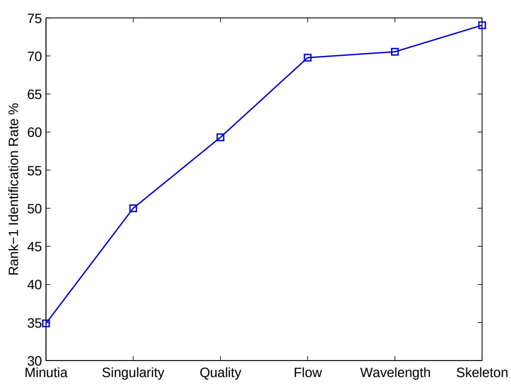

(a)

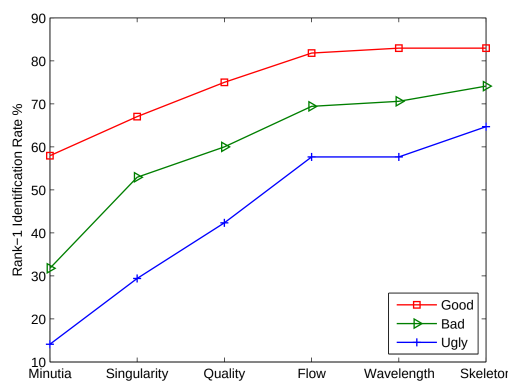

(b)

Fig. 11. Plot of rank-1 identification rates vs. features. (a) All 258 latents, (b) Good, Bad and Ugly quality latent prints.

mated rolled print. In this example, with the incremental use of extended features, the rank of the mated rolled print is 206 (minutiae), 114 (singularity), 5 (quality), 2 (flow), 2 (wavelength), and 1 (skeleton), respectively.

E. Secondary Features (Level 3 Features)

To evaluate the potential effect of secondary features on matching accuracy, following experiment was conducted. A latent expert was asked to manually mark the pores, dots and incipients in all the 258 latents and the mated rolled prints in SD27. The histograms of these secondary

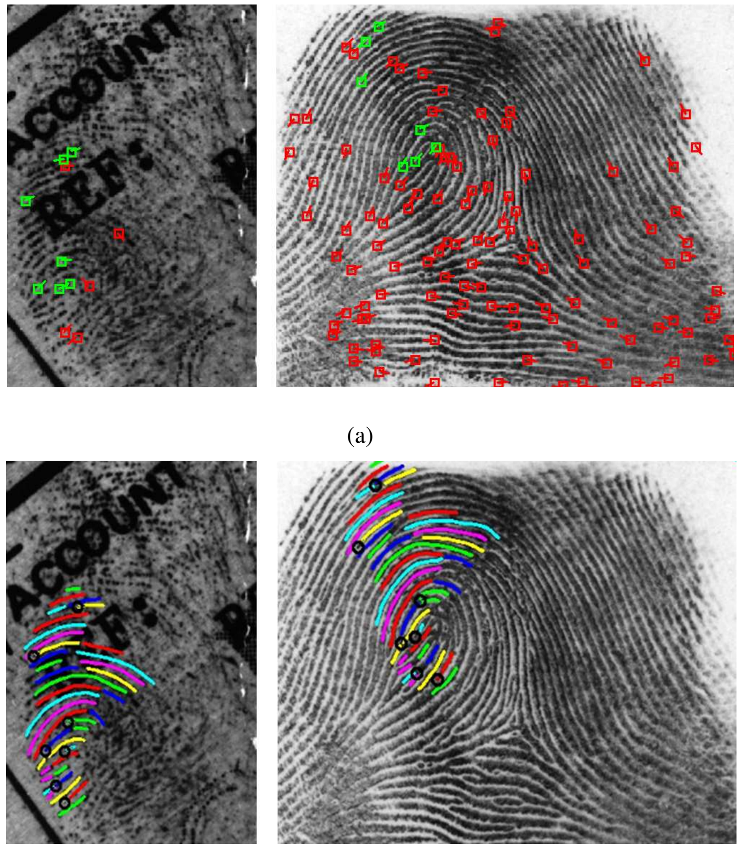

(a)

(b)

Fig. 12. The matching result of a pair of mated fingerprints. (a) Minutiae matching, (b) skeleton matching.

features are shown in Fig. 13. The dots and incipients are marked by the latent expert as line segments. We divide the length by the average ridge wavelength (10 pixels) to represent the number of dots/incipients. To evaluate the repeatability of these features in both latents and rolled prints, we align mated fingerprints using the ground-truth mated minutiae provided by NIST and count the number of mated features (a pair of feature points is deemed as mated if their distance is less than 16 pixels). The histograms of mated secondary features in 258 pairs of fingerprints as shown in Fig. 13. It can be observed that: 1) only 15 latents have more than 20 pores and only 4 latents have more than 20 mated pores; 2) only 5 latents have more than 5 dots/incipients and only 2 latents have more than 5 mated dots/incipients. In the case of automatic feature extraction, the repeatability of these features will be even lower. The utility of secondary features, at least for this database, is further diminished if we consider the following

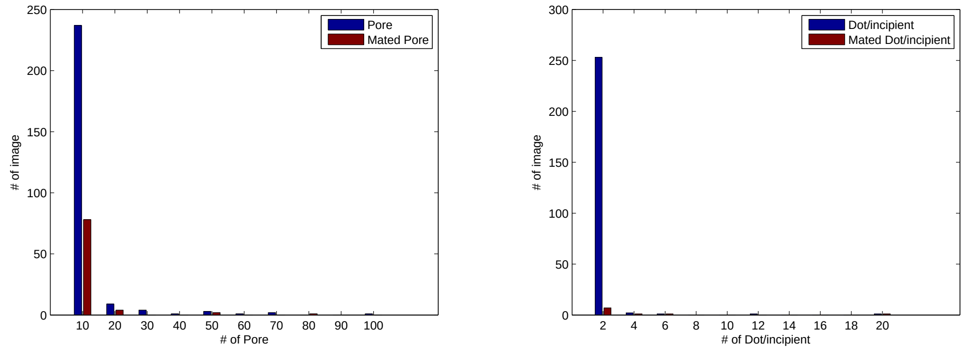

(a) (b)

Fig. 13. Histograms of the ground-truth secondary features in NIST SD27. (a) Pores and mated pores, (b) dots/incipients and mated dots/incipients.

facts: 1) they are highly correlated with skeleton, which has already been used in our matching algorithm; 2) they tend to appear more in good quality latents, which can be easily identified by the minutiae matcher. For instance, the latent in Fig. 2 and its mated rolled print have the maximum number (20) of mated dots/incipients in SD27. However, its mated rolled print has already been correctly identified at rank-1 by the minutiae matching algorithm. Taking all these observations into account, we can conclude that using secondary features will not lead to obvious improvement in the matching accuracy at least in the NIST SD27 database. This conclusion also holds even if these fingerprints are scanned at 1000 ppi, since the histograms in Fig. 13 are based on the ground-truth features marked by a latent expert who can reliably detect secondary features at 500 ppi.

F. Speed

The experiments were conducted on a PC with Intel Core2 Duo CPU and Windows XP operating system. The automatic feature extraction takes 580 ms for a rolled print in NIST SD4 and 735 ms for a print in NIST SD27 and SD14. It takes around eight minutes to match a latent against all the 29,257 rolled prints.

V. Conclusions and Future Work

We have proposed a system for matching latent fingerprints with rolled fingerprints. The matching module consists of minutiae matching, orientation field matching, and skeleton matching. To test the proposed system, 258 latent fingerprints in NIST SD27 are matched against a background database consisting of 29,257 rolled fingerprints from three different NIST databases. The rank-1 identification rate of 34.9% of the baseline minutiae matcher was improved to 74%, when singularity, ridge quality map, ridge flow map, ridge wavelength map and skeleton are incrementally used. The importance of various extended features has also been studied and the experimental results indicate that singularity, ridge quality map and ridge flow map are the most effective features in improving the matching accuracy.

The proposed latent matching algorithm is still inferior to the performance of experienced latent examiners, which may be caused by three major differences between the methodologies used by latent experts and automatic matchers.

- Approaches used in matching ridge skeleton and minutiae (or Level 2 features) are different. Latent examiners employ a "ridges in sequence" method [47] in the matching process, which is robust to noise and distortion. While the proposed skeleton matching algorithm tries to mimic such a method, it is not robust in the presence of large amounts of noise and distortion. The minutiae matching algorithm is also prone to spurious minutiae and distortion.
- The approach used to match the detailed ridge features (or Level 3 features) is different. When latent examiners compare the detailed ridge features in fingerprints, there is no explicit separation between feature extraction and matching stages. The separation of feature extraction and matching in automatic systems leads to some information loss. In addition, the automatic feature extractor may not be able to extract Level 3 features from rolled prints that are always compatible with the features marked by latent examiners.
- The approach to utilizing negative evidence is different. Latent examiners can determine a pair of fingerprints as unmatched based on a single unmatched minutia which is located in the good quality region of the two fingerprints. This is a risky proposition for fingerprint algorithms.

We plan to improve the latent matching accuracy by reducing these differences.

Manual feature markings for poor quality latent fingerprints is a time consuming and tedious task. Considering that latent examiners often have to process many latents within a limited time period, significant attention should be paid to the automatic latent feature extraction problem. Given the performance gap between automatic and semi-automatic latent matching systems, human intervention is likely to be necessary for some time. One way to reduce manual processing is to define a latent fingerprint quality measure, which is continuously updated when latent examiners are marking features. Once the quality measure reaches a predefined threshold, the latent examiners are notified that the image quality is already good enough to perform a latent search.

Acknowledgments

The authors would like to acknowledge the assistance of Lt. Gregoire Michaud and Sgt. Scott Hrcka of the Forensic Science Division of Michigan State Police and Austin Hicklin of Noblis. This work was supported by research grants US Army Research Office W911NF-06-1-0418 and US National Institute of Justice 2007-RG-CX-K183.

References

[1] A. K. Jain, J. Feng, A. Nagar, and K. Nandakumar, "On Matching Latent Fingerprints," in *Proc. CVPR Workshop on Biometrics*, June 2008, pp. 1–8.

[2] P. Komarinski, *Automated Fingerprint Identification Systems (AFIS)*. Elsevier Academic Press, 2005.

[3] H. C. Lee and R. E. Gaensslen, Eds., *Advances in Fingerprint Technology*. CRC Press, 2001.

[4] C. Champod, C. Lennard, P. Margot, and M. Stoilovic, *Fingerprints and Other Ridge Skin Impressions*. CRC Press, 2004.

[5] "Fingerprint Minutiae from Latent and Matching Tenprint Images," NIST Special Database 27, http://www.nist.gov/srd/nistsd27.htm.

[6] D. R. Ashbaugh, *Quantitative-Qualitative Friction Ridge Analysis: An Introduction to Basic and Advanced Ridgeology*. CRC Press, 1999.

[7] A. A. Moenssens, "Is Fingerprint Identification a Science?" Forensic-Evidence.com, 1999, http://forensic-evidence.com/site/ID/ID00004_2.html.

[8] M. J. Saks and J. J. Koehler, "The Coming Paradigm Shift in Forensic Identification Science," *Science*, vol. 309, August 2005.

[9] L. Haber and R. N. Haber, "Error rates for human latent fingerprint examiners," in *Automatic Fingerprint Recognition Systems*, N. Ratha and R. Bolle, Eds. Springer-Verlag, 2003, ch. 17, pp. 339–360.

[10] "A Review of the FBI's Handling of the Brandon Mayfield Case," Office of the Inspector General, Special Report, March 2006, http://www.usdoj.gov/oig/special/s0601/PDF_list.htm.

[11] Case Profile, Innocence Project, http://www.innocenceproject.org/Content/73.php.

[12] S. A. Cole, "More than Zero: Accounting for Error in Latent Fingerprint Identification," *Journal of Criminal Law and Criminology*, vol. 95, no. 3, pp. 985–1078, 2005.

[13] "Conclusion of circuit court judge Susan Souder - grants motion to exclude testimony of forensic fingerprint examiner - capital murder case: State of Maryland v. Bryan Rose," October 2007, http://www.clpex.com/Information/STATEOFMARYLAND-v-BryanRose.doc.

[14] V. N. Dvornychenko and M. D. Garris, "Summary of NIST Latent Fingerprint Testing Workshop," NISTIR 7377, November 2006, http://fingerprint.nist.gov/latent/ir_7377.pdf.

[15] C. Wilson, "Fingerprint Vendor Technology Evaluation 2003: Summary of Results and Analysis Report," NISTIR 7123, June 2004, http://fpvte.nist.gov/report/ir_7123_analysis.pdf.

[16] "Evaluation of Latent Fingerprint Technologies 2007," http://fingerprint.nist.gov/latent/elft07/.

[17] CDEFFS: The ANIS/NIST Committee to Define an Extended Fingerprint Feature Set, http://fingerprint.nist.gov/standard/cdeffs/index.html.

[18] "American National Standard for Information Technology - Finger Minutiae Format for Data Interchange," ANSI/INCITS 378-2004, 2004, http://www.incits.org.

[19] "NIST 8-Bit Gray Scale Images of Fingerprint Image Groups (FIGS)," NIST Special Database 4, http://www.nist.gov/srd/nistsd4.htm.

[20] "NIST Mated Fingerprint Card Pairs 2 (MFCP2)," NIST Special Database 14, http://www.nist.gov/srd/nistsd14.htm.

[21] The NAS Committee on Identifying the Needs of the Forensic Science Community, "Strengthening Forensic Science in the United States: A Path Forward," National Academy of Sciences, 2009, http://www.nap.edu/catalog.php?record_id=12589.

[22] FBI Electronic Fingerprint Transmission Specification, http://www.fbi.gov/hq/cjisd/iafis/efts71/efts71.pdf.

[23] P. Lo and B. Bavarian, "Expert Matcher Fingerprint System," US Patent No. 5,960,101, 1999.

[24] M. Hara and H. Toyama, "Method and Apparatus for Matching Streaked Pattern Image," US Patent No. 7,295,688, 2007.

[25] NIST Minutiae Interoperability Exchange Test (MINEX), http://fingerprint.nist.gov/minex04/.

[26] NIST Proprietary Fingerprint Template (PFT) Testing, http://fingerprint.nist.gov/pft/.

[27] R. M. McCabe and M. D. Garris, "Summary of April 2005 ANSI/NIST Fingerprint Standard Update Workshop," NISTIR 7242, July 2005, http://fingerprint.nist.gov/standard/archived_workshops/workshop1/ir7242.pdf.

[28] SWGFAST, Scientific Working Group on Friction Ridge Analysis, Study and Technology, http://www.swgfast.org.

[29] CDEFFS, Data Format for the Interchange of Extended Fingerprint and Palmprint Features, WORKING DRAFT Version 0.2, January 2008, http://fingerprint.nist.gov/standard/cdeffs/Docs/CDEFFS_DraftStd_v02_2008-01-18.pdf.

[30] J. Feng, "Combining Minutiae Descriptors for Fingerprint Matching," *Pattern Recognition*, vol. 41, no. 1, pp. 342–352, 2008.

[31] M. Tico and P. Kuosmanen, "Fingerprint Matching Using an Orientation-based Minutia Descriptor," *IEEE Trans. Pattern Analysis and Machine Intelligence*, vol. 25, no. 8, pp. 1009–1014, 2003.

[32] J. Gu, J. Zhou, and C. Yang, "Fingerprint Recognition by Combining Global Structure and Local Cues," *IEEE Trans. Image Processing*, vol. 15, no. 7, pp. 1952–1964, 2006.

[33] P. Lo and G. Yu, "Print Matching Method and System Using Direction Images," US Patent Application Publication No. 2008/0273769A1, 2008.

[34] A. K. Jain, Y. Chen, and M. Demirkus, "Pores and Ridges: High-Resolution Fingerprint Matching Using Level 3 Features," *IEEE Trans. Pattern Analysis and Machine Intelligence*, vol. 29, no. 1, pp. 15–27, 2007.

[35] D. Wan and J. Zhou, "Fingerprint Recognition Using Model-based Density Map," *IEEE Trans. Image Processing*, vol. 15, no. 6, pp. 1690–1696, 2006.

[36] J. Feng, Z. Ouyang, and A. Cai, “Fingerprint Matching Using Ridges,” *Pattern Recognition*, vol. 39, no. 11, pp. 2131 – 2140, 2006.

[37] A. K. Jain, L. Hong, and R. M. Bolle, “On-line Fingerprint Verification,” *IEEE Trans. Pattern Analysis and Machine Intelligence*, vol. 19, no. 4, pp. 302–314, 1997.

[38] J. Zhou, F. Chen, N. Wu, and C. Wu, “Crease Detection from Fingerprint Images and Its Applications in Elderly People,” *Pattern Recognition*, 2008.

[39] J. D. Stosz and L. A. Alyea, “Automated System for Fingerprint Authentication Using Pores and Ridge Structure,” in *Proc. SPIE Conf. Automatic Systems for the Identification and Inspection of Humans*, vol. 2277, no. 1, 1994, pp. 210–223.

[40] International Biometric Group (IBG), “Analysis of Level 3 Features at High Resolutions: Phase II - Final Report,” Tech. Rep., 2008.

[41] Y. Chen and A. K. Jain, “Dots and Incipients: Extended Features for Partial Fingerprint Matching,” in *Proc. Biometrics Symposium*, September 2007, pp. 1–6.

[42] Neurotechnology Inc., VeriFinger, http://www.neurotechnology.com.

[43] Q. Xiao and H. Raafat, “Fingerprint Image Postprocessing: Combined Statistical and Structural Approach,” *Pattern Recognition*, vol. 24, no. 10, pp. 985 – 992, 1991.

[44] D. Maltoni, D. Maio, A. K. Jain, and S. Prabhakar, *Handbook of Fingerprint Recognition*. Springer-Verlag, 2003.

[45] Z. Kovacs Vajna, “A Fingerprint Verification System Based on Triangular Matching and Dynamic Time Warping,” *IEEE Trans. Pattern Analysis and Machine Intelligence*, vol. 22, no. 11, pp. 1266–1276, 2000.

[46] X. Chen, J. Tian, and X. Yang, “A New Algorithm for Distorted Fingerprints Matching Based on Normalized Fuzzy Similarity Measure,” *IEEE Trans. Image Processing*, vol. 15, no. 3, pp. 767–776, 2006.

[47] SWGFAST, Memo to Mike McCabe (NIST) Regarding ANSI/NIST ITL 1-2000, November 2005, http://fingerprint.nist.gov/standard/cdeffs/Docs/SWGFAST_Memo.pdf.

[48] J. Feng, S. Yoon, and A. K. Jain, “Latent Fingerprint Matching: Fusion of Rolled and Plain Fingerprints,” in *Proc. 2nd International Conference on Biometrics (ICB) (to appear)*, June 2009.